Reprinted from

APPLIED GEOPHYSICS

Journal of Applied Geophysics 35 (1996) 79–87

Interface waves propagated along a fracture

Laura J. Pyrak-Nolte *, Sanjit Roy, Beth L. Mullenbach

Department of Civil Engineering and Geological Sciences, University of Notre Dame, Notre Dame, Indiana 46556-0767, USA

ELSEVIER

ELSEVIER

Journal of Applied Geophysics 35 (1996) 79–87

JOURNAL OF APPLIED GEOPHYSICS

Interface waves propagated along a fracture

Laura J. Pyrak-Nolte *, Sanjit Roy, Beth L. Mullenbach

Department of Civil Engineering and Geological Sciences, University of Notre Dame, Notre Dame, Indiana 46556-0767, USA

Abstract

The existence of interface waves along fractures depends on the specific stiffness of the fracture. With increasing fracture stiffness, the velocity of the interface wave increases and the spectral content of the signal is altered. We used interface wave measurements and wavelet analysis to examine the effect of normal and shear stresses on fracture shear stiffness. Fracture shear stiffness is more sensitive to changes in shear stress than to normal stress.

Compressional waves propagated along a fracture appear to contain a delayed wave that is sensitive to changes in the fracture stiffness. Using acoustic wavefront imaging, we are able to visualize the delayed produced in the compressional-wave by the fracture from the spatial distribution of the arriving energy.

1. Introduction

Rock masses contain fractures and discontinuities on all length scales that affect the mechanical stability and the flow of fluids through it. A goal of site characterization for mineral exploration or waste isolation is to detect and characterize the hydraulic and mechanical properties of fractures using seismic techniques. A difficulty in interpreting seismic data from fractured rock masses arises from the conversion of waves at fractures, which include interface waves. Pyrak-Nolte and Cook (1987) predicted, using the displacement discontinuity model, the existence of elastic interface waves that propagate along a fracture. In this model, the fracture is represented as a non-welded contact, i.e., the stress across the fracture is continuous but the displacements are discontinuous. The discontinuity in displacement is inversely proportional to the fracture specific stiffness, which is the ratio of an increment in stress to the resulting increment in displacement produced by the deformation of the void space within the fracture. From the displacement-discontinuity theory, two elastic interface waves are shown to exist: (1) the fast interface which depends only on the normal specific stiffness of the fracture; and (2) the slow wave which depends only on the shear stiffness of the fracture. These waves are distinct eigenmodes that can be thought of as coupled Rayleigh waves that are coupled through the points of contact in the fracture. The fast and slow interface waves are characterized by negative velocity dispersion (Pyrak-Nolte and Nolte, 1995) and by velocities that range between the bulk shear-wave velocity and the Rayleigh wave velocity depending on the fracture specific stiffness. These waves have been shown to exist on synthetic fractures in aluminum (Pyrak-Nolte et al., 1992) and induced fractures in rock (Ekern et al., 1995; Roy and Pyrak-Nolte, 1995).

Several investigators have shown that fracture specific stiffness depends on the geometry of the

* Tel.: 219-631-8377; fax: 219-631-9236; e-mail: pyrak-nolte@.nd.edu.

PII S0926-9851(96)00009-2

void space in the fracture (Hopkins et al., 1987; Hopkins et al., 1990) and on the roughness of the fracture surfaces (Brown and Scholz, 1985; Brown and Scholz, 1986; Yoshioka and Scholz, 1989). The geometry of the fracture, in turn, is affected by the processes that formed the fracture, as well as processes that alter the fracture properties, such as lithostatic stress and weathering. In this paper, we present research on the characterization of fracture stiffness using interface waves and wavelet signal analysis. In addition, we present data that suggests that the first-arriving compressional wave energy also contains information concerning changes in stiffness of a fracture subjected to stress.

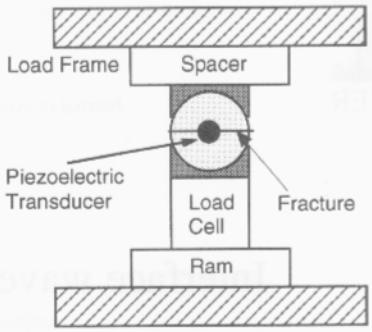

Fig. 1. Sketch of experimental set-up for measuring interface waves under load.

2. Experimental set-up

2.1. Interface waves

Laboratory measurements of interface waves in three dolomite cores were made to determine the change in the shear stiffness of fractures subjected to both normal and shear stresses. The dimensions and density of samples A, B, and C are listed in Table 1. Initial measurements of the velocity and amplitude of compressional (P) and shear (S) waves were made on intact samples, i.e., prior to inducing a fracture.

A sketch of the experimental set-up is shown in Fig. 1. A cylindrical sample is placed in a loading frame, and piezoelectric transducers with a center frequency of 1.0 MHz were clamped on the sample (straddling the center line on the intact samples) for sending and receiving the transmitted waves. For the intact sample, the shear-wave polarization was oriented parallel to the direction of loading. After characterizing the intact samples, fractures were induced in the cores using a technique similar to Brazil testing (Jaeger and Cook, 1979) or split-cylinder testing. For the fractured samples, the shear-wave polarization was oriented perpendicular to the fracture plane and the transducers were mounted straddling the fracture. For the effect of fractures on shear waves with the polarization oriented parallel to the fracture plane, the reader is referred to Roy and Pyrak-Nolte (1995).

Data were collected as a function of stress (0.03 MPa to 11.5 MPa) for the fractured and intact samples. The effect of shear stress on fracture stiffness was examined by orienting the fracture at an acute angle to the direction of loading. The orientation of the fracture relative to the normal load is given in Table 1. Under shear loading, the sample was constrained to prevent slippage along the fracture. For all measurements, the transducers were excited with a 250 V square pulse with a width of 0.4 μs and a repetition rate of 100 Hz. The data were collected on a digital oscilloscope and stored on a computer. The

Table 1
Density, dimensions, bulk wave velocities, and spectral peak of interface waves for dolomite samples A, B, and C, and oolitic limestone samples G and H

	Sample				
	A	B	C	G	H
Diameter (cm)	5.05	5.06	5.05	5.05	5.04
Length (cm)	5.00	4.91	4.83	7.18	7.19
Density (kg/m)	2701	2678	2714	2346	2332
Angle of fracture relative to normal load	30°	7.5°	52.5°	–	–
Intact compressional-wave velocity (m/s)	5554	5575	5676	4770	4581
Intact shear-wave velocity (m/s)	3278	3298	3386	2638	2538

effect of fractures on compressional waves was investigated using intact (G) and fractured (H) samples of oolitic limestone.

3. Results

3.1. Waveforms from interface wave experiments

Measurements of compressional and shear-waves propagated through the intact samples were made to characterize the seismic properties of the intact samples as a function of stress. The received waveforms for intact sample A are shown in Fig. 2 for a range of normal stresses (0.25–8.72 MPa). The shear-wave arrival time and amplitude did not change with increasing normal stress which is consistent with the lack of pore structure in the dolomite samples.

After single fractures were induced in the intact samples, measurements of shear-wave amplitudes and velocities were made to determine the effect of normal stress on the shear stiffness of a fracture by measuring the slow interface-wave. The velocity of the slow interface-wave is controlled by the shear stiffness of the fracture (Pyrak-Nolte and Cook, 1987) but is independent of the normal stiffness. The received waveforms for *fractured* sample A are given

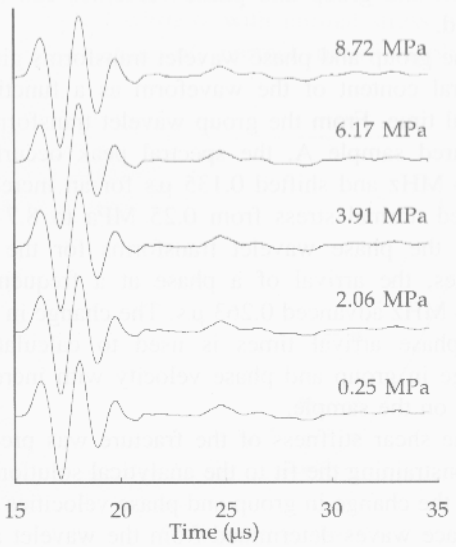

Fig. 2. Received shear-waves for intact sample A for a range of stresses

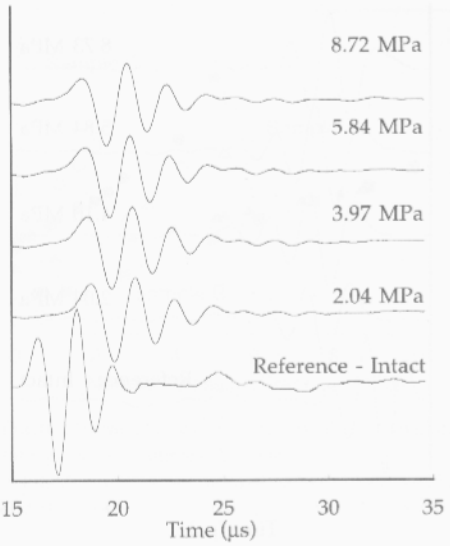

Fig. 3. Interface waves measured on fractured sample A for normal stresses ranging from 2.04 MPa to 8.72 MPa. A shear-wave measured on intact sample A is shown for comparison.

in Fig. 3 and show that all of the energy is coupled into the slow interface wave with no detectable fast interface-wave or bulk shear-wave. A waveform from *intact* sample A is also shown in Fig. 3 for comparison to illustrate the difference in the arrival times of the shear wave and the interface wave. The slow interface-wave is delayed 2.14 μs relative to the shear-wave in the intact sample and the high frequency components of the signal are attenuated. This delay in the interface wave cannot be described as simply an effect of anisotropy produced by the presence of a fracture or by shear-wave birefringence. The interface wave is a distinct eigenmode localized at the fracture plane with distinct characteristics. For example, analysis of the particle motion of the interface wave shows that it contains both transverse and longitudinal motions similar to that of a Rayleigh wave, which is predicted from the interface wave theory (Pyrak-Nolte and Cook, 1987; Gu, 1994).

An important aspect of how the interface wave depends on fracture specific stiffness can be demonstrated by applying increasing normal stress. It is important to point out that although the slow interface-wave depends only on shear stiffness, that stiffness increases with increasing normal stress because of the increase in contact area between the two

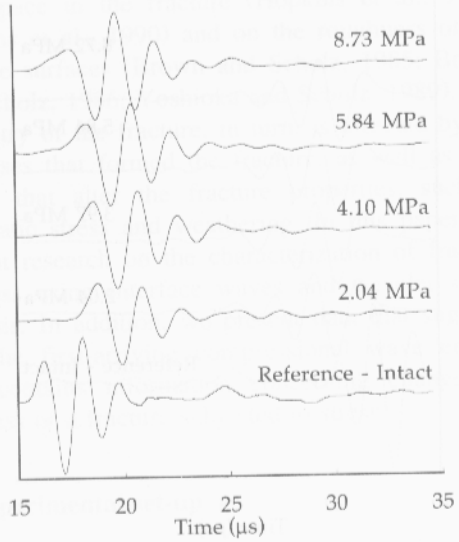

Fig. 4. Interface waves measured on fractured sample A when both a normal and a shear stress are applied to the fracture. A shear-wave measured on intact sample A is shown for comparison. Stresses in figure are the normal stresses on the fracture plane.

fracture surfaces. Therefore as normal stress is increased on the sample (Fig. 3), the interface-wave arrival shifts to earlier times and the amplitudes of the successive antinodes increase and/or decrease as the stiffness of the fracture increases.

As we illustrated above, normal stress increases the shear stiffness of the fracture. However, we also investigated the effect of shear stress on the fracture shear stiffness. Therefore, we simultaneously applied a normal and a shear stress to the fracture by orienting the fracture at an acute angle to the normal load. Fig. 4 shows the received waveforms for *fractured* sample A when both normal and shear stresses are applied to the fracture plane. An *intact* sample A waveform is shown for comparison. The stresses given in Fig. 3 and Fig. 4 are the normal stresses on the fracture plane. The effect of shear stress on the slow interface-wave is directly observable in the waveforms as a dramatic shift in both phase and group velocity, which is reflected by the change in amplitudes of the successive antinodes as they move within the wave envelope. To extract quantitative values for the increase in fracture stiffness with increasing stress, we applied a wavelet analysis of the seismic waveforms.

4. Wavelet analysis of interface waves

The group and phase velocities of the slow interface-wave depend on the shear stiffness of the fracture and range between the bulk shear-wave velocity and the Rayleigh-wave velocity (Pyrak-Nolte and Cook, 1987). Slow interface-waves propagated along very compliant fractures travel at the Rayleigh velocity because the two fracture surfaces are behaving as if they were uncoupled, i.e., as free surfaces. For fractures with very high stiffness, the slow interface wave travels at the bulk shear-wave velocity because the fracture is behaving as if it were a welded contact. To determine the shear stiffness of the fracture from the slow interface wave data, it is necessary to quantify the changes in group and phase velocity. We performed a wavelet analysis of the measured interface waves to provide a direct quantitative measure of the group velocity and changes in phase velocity of the observed interface waves. In our analysis, a Morlet wavelet transform (Morlet et al., 1982; Pyrak-Nolte and Nolte, 1995) is applied to the received waveforms to produce both a group and a phase wavelet transform from which the spectral content and group and phase velocities can be extracted.

The group and phase wavelet transforms give the spectral content of the waveform as a function of arrival time. From the group wavelet transforms for fractured sample A, the spectral peak occurred at 0.944 MHz and shifted 0.135 μs for an increase in applied normal stress from 0.25 MPa to 8.7 MPa. From the phase wavelet transforms for the same stresses, the arrival of a phase at a frequency of 0.944 MHz advanced 0.263 μs. The change in group and phase arrival times is used to calculate the change in group and phase velocity with increasing stress on the sample.

The shear stiffness of the fracture was predicted by constraining the fit to the analytical solution (Fig. 5) by the change in group and phase velocities of the interface waves determined from the wavelet analysis. The change in group velocity and phase velocity (based on the analysis of the data from the minimum

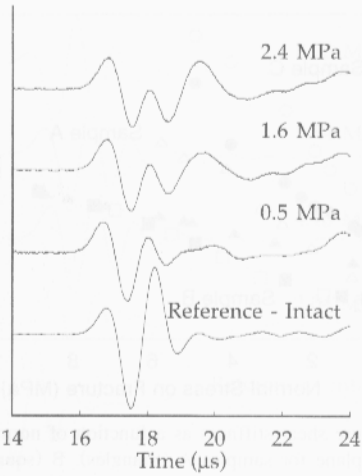

Fig. 7. Compressional waveforms collected for fractured sample H for a range of stresses. A waveform from intact sample G is shown for comparison.

fractures and joints in rocks, which may make it difficult to use interface waves for fracture characterization. The primary or first-arriving compressional (P) wave is often easier to measure in the field. However, the effect of fractures on compressional waves propagated parallel to a fracture has not been quantified and is not well understood. Here, we present results from experiments to examine the behavior of compressional waves propagated parallel to a fracture.

5.1. Compressional waveforms

Measurements of compressional waves were made on an intact (sample G) and a fractured (sample H) specimen of oolitic limestone. The dimensions of the samples are given in Table 1. The experimental method is the same as that described in Section 2.1 above except compressional-mode piezoelectric transducers were used to send and receive the signal. Fig. 7 contains the received compressional wave forms for the fractured sample for three stresses applied normal to the fracture plane. In addition, a waveform from the intact sample is shown for comparison to illustrate the difference in the arrival times and in the frequency content of the compressional wave propagated through an intact sample compared with a fractured sample. On the fractured sample, the compressional-wave broadens with increasing stress indicating a shift in energy to lower frequencies and the emergence of a delayed wave. The delayed wave can be seen in the waveform for a stress of 2.4 MPa. Wavelet analysis of compressional waves propagated through sample H showed a shift in the frequency content of 0.305 MHz and an increase in arrival time of 1.255 μs for a stress change of 1.9 MPa.

5.2. Acoustic wavefront imaging of the effect of a fracture on compressional waves

A delayed wave was observed to propagate with speeds near the bulk compressional-wave velocity as waves were propagated parallel to a fracture (Fig. 7). Gu (1994) predicted the existence of a leaky mode interface wave that propagates with a velocity between the bulk shear-wave velocity and the bulk-compressional wave velocity, that exhibits both transverse and longitudinal particle motions, and that leaks energy away from the fracture into the surrounding medium. Further investigation is needed to determine if the experimental observation described above (Section 5.1) is the leaky-mode interface-wave. However, by using an acoustic wavefront imaging technique, we explored the spatial distribution of energy from compressional waves propagated parallel to a fracture.

An acoustic wavefront imaging technique similar to Wolfe (1995) was used to image the spatial distribution of compressional wave energy propagated through an intact and a fractured sample of dolomite. The sample measured 9.1 cm in diameter by 9.3 cm in length. The waves were propagated along the axis of the intact sample and parallel to the fracture for the fractured sample. Measurements were made initially on an intact sample, after which a fracture was induced in the sample, as described in Section 2.1. The acoustic wavefront imaging technique uses water-coupled spherically-focused piezoelectric (0.5 MHz) transducers to send and receive the signal. The sample was sealed and placed in a distilled water-filled tank. The source transducer was fixed in position while the receiving transducer scanned a 60 mm by 60 mm area in 1 mm increments recording a 50 μs window of the waveform at each position. This technique results in a three-di-

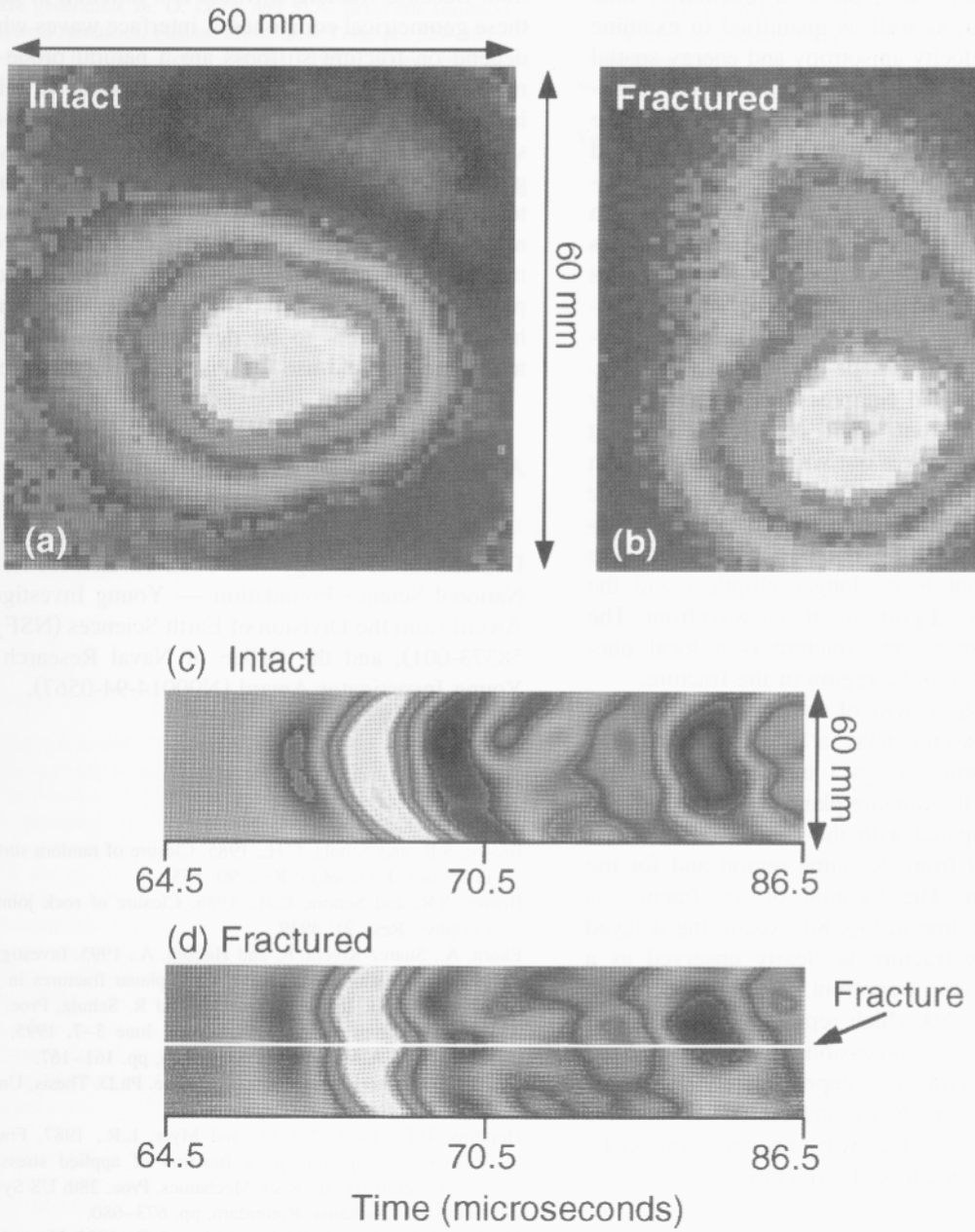

Fig. 8. Spatial distribution of arriving compressional wavefront for the (a) intact and (b) fractured sample for an arrival time of 67.5 μs. The colors in (a) and (b) represent nodes and antinodes of constant amplitude. The received compressional waveforms along a vertical line perpendicular to the fracture (d) and from the companion intact sample (c) are shown. In (c) and (d) the colors represent the amplitudes of the nodes and antinodes of the wave train, with blue representing the lowest amplitudes and yellow representing the highest amplitudes. The compressional wavefront is delayed by the fracture as observed by the "notch" in the wavefront in (d) and the indentation in the contours in (b).

mensional data set, i.e., 60 mm by 60 mm by 50 μs (0.05 μs/point). Using computer visualization techniques, the arriving wavefront as a function of time can be visualized, as well as quantified to examine such issues as velocity anisotropy and energy spatial distribution in rock and sediment samples. For example, Fig. 8a and Fig. 8b are contour plots of the arriving compressional wavefront from the intact and the fractured sample. The image represents the distribution of the wavefront over a 60 mm by 60 mm region of the sample for an arrival time of 67.5 μs with the colors representing the nodes and antinodes of the wave. The natural anisotropy in compressional-wave velocity of the dolomite samples is exhibited by the elliptical shape of the wavefront (Fig. 8a). If the sample had compressional-wave velocity isotropy, the wavefront would be circular showing that the wavefront moves out with an equal speed in all directions. For the fractured sample, the time delayed caused by the fracture appears as an indentation or "notch" in the contours (Fig. 8b). The arriving wavefront is no longer elliptical and the fracture has delayed portions of the wavefront. The delayed produced by the fracture is a local phenomenon confined to the region of the fracture.

To quantify the extent of the region around the fracture that causes the delay, a 12 μs window of the received waveforms over a 1 mm by 60 mm strip perpendicular to the fracture plane is shown (Fig. 8d) and can be compared with the data from the intact sample (Fig. 8c) from the same region and for the same orientation. The location of the fracture is given by a white line in Fig. 8d. Again, the delayed produced by the fracture is clearly observed as a notch in the arriving wavefront. The notched region at 67.5 μs (Fig. 8d) which represents the effect of the fracture on the compressional wave, is localized to a 3–4 mm region, i.e., approximately the wavelength of the signal. Nagy and Adler (1991) have theorized that the interface wave phenomenon occurs within one wavelength of the fracture.

6. Summary

In summary, fractures in rocks can support eigenmodes that travel along a fracture with distinct velocity, amplitude and spectral behavior which are directly related to the geometry of the fracture, that is the contact area, void shape and void spatial distribution. Because fracture stiffness is a function of all of these geometrical components, interface waves which depend on fracture stiffness are a natural probe for monitoring the condition of a fracture. The initial investigation on the effect of fractures on compressional waves propagated parallel to a fracture suggests that the first arrival of signal can also be used to monitor fracture stiffness but further investigation needs to be performed to determine the exact relationship between the fracture stiffness and this compressional-mode interface-wave. Interface waves have the potential to be developed into a seismic technique for field use for characterizing fractures.

Acknowledgements

The LJPN wishes to acknowledge D.D. Nolte, the Department of Energy (DE-F602-93 ER14391), the National Science Foundation — Young Investigator Award from the Division of Earth Sciences (NSF/94 58373-001), and the Office of Naval Research — Young Investigator Award (N00014-94-0567).

References

Brown, S.R. and Scholz, C.H., 1985. Closure of random surfaces in contact. J. Geophys. Res., 90: 5531.

Brown, S.R. and Scholz, C.H., 1986. Closure of rock joints. J. Geophys. Res., 91: 4939.

Ekern, A., Suarez-Rivera, R. and Hansen, A., 1995. Investigation of interface wave propagation along planar fractures in sedimentary rocks. In: J.J.K. Daemen and R. Schulz, Proc. 35th US Symposium on Rock Mechanics, June 5–7, 1995, Lake Tahoe, CA. A.A. Balkema, Rotterdam, pp. 161–167.

Gu, B., 1994, Interface waves on a fracture. Ph.D. Thesis, University of California, Berkeley.

Hopkins, D.L., Cook, N.G.W. and Myer, L.R., 1987. Fracture stiffness and aperture as a function of applied stress and contact geometry. In: Rock Mechanics, Proc. 28th US Symposium. A.A. Balkema, Rotterdam, pp. 673–680.

Hopkins, D.L., Cook, N.G.W. and Myer, L.R., 1990. Normal joint stiffness as a function of spatial geometry and surface roughness. In: N. Barton and O. Stephansson (Editors), Proc. Int. Symp. Rock Joints. A.A. Balkema, Rotterdam, pp. 203–210.

Jaeger, J.C. and Cook, N.G.W., 1979. Fundamentals of Rock Mechanics. Pergamon Press, New York.

Morlet, J., Arens, G., Fourgeau, E. and Giard, D., 1982. Wave